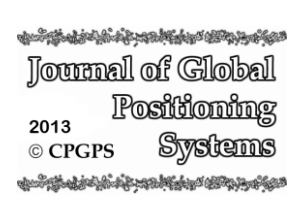
Journal of Global Positioning Systems (2013)

Vol.12, No.1 : 53-60 DOI: 10.5081/jgps.12.1.53



# Stochastic Ionosphere Models for Precise GNSS Positioning: Sensitivity Analysis

## Peiyuan Zhou and Jinling Wang

School of Civil and Environmental Engineering, University of New South Wales, Sydney, NSW 2052, Australia

#### **Abstract**

In Global Navigation Satellite System (GNSS) positioning, ranging signals are delayed when travelling through the ionosphere, the layer of the atmosphere ranging in altitude from about 50 to 1000 km consisting largely of ionized particles. This delay can vary from 1 meter to over 100 meters, and is still one of the most significant error sources in GNSS positioning. In precise GNSS positioning applications, ionospheric errors must be accounted for. One way to do so is to treat unknown ionosphere delay as stochastic parameter, which can account for the ionospheric errors in the GNSS measurements as well as keeping the full original information. The idea is adding ionospheric delay from external sources as pseudo-observables. In this paper, the performance of ionosphere-weighted model is evaluated using real data sets, and the correctness of priori ionosphere variance is also validated.

Keywords: GNSS, Ionospheric Error, Stochastic Model

#### 1. Introduction

For the past several decades, carrier phase-base precise positioning is essential for a wide range of applications. And more and more users are gaining interest in medium or long-range precise positioning methods. However, in a conventional RTK (real time kinematic) positioning process, the distance between a rover and a reference station is often limited to 10-30 kilometres (Hu et al., 2005). The main factors causing this limitation are some distance-dependent errors, such as atmospheric refractions, especially the ionosphere error, satellite orbit error and clock biases. As ionospheric delay is spatial correlated and this spatial correlation decreases with the increasing distance of baseline, ionosphere effects are hard to be cancelled by DD (double-difference) (Wielgosz, 2011). Failure to deal with ionospheric errors properly will disrupt ambiguity resolution process significantly as well as the final baseline solution (Takasu and Yasuda, 2010). As a result, ionospheric

errors cannot be neglected in medium or long-range baseline processing.

In order to resolve integer ambiguities in carrier phases reliably and robustly, ionospheric errors have to be kept as small as possible. There have been investigations to develop stochastic ionospheric models, which can account for the stochastic behaviors of ionosphere in the measurements as well as keeping the full original information. Some work has been conducted to treat ionosphere as stochastic parameters. One of the most popular methods is based on ionosphere-weighted model, in which the double-differenced ionospheric delays are treated stochastically instead of deterministically (Odijk, 2000, Liu, 2001, Alves et al., 2002, Odijk, 2002). By adding external ionospheric information into the original observation equations, the model strength is improved. And this improvement can contribute to the ambiguity resolution process (Teunissen, 1997a, Teunissen, 1997b). The ionospheric pseudo-observables can be obtained from ionosphere models, such as Klobuchar model (Klobuchar, 1987), GIM (Global Ionosphere Maps) (Schaer et al., 1995, Mannucci et al., 1998, Schaer, 1999). For shorter baselines, this sample value may even be set as zero.

However, estimation of the ionosphere delay is only optimal if a correct stochastic model is chosen for this parameter. For conventional pseudorange and carrier phase measurements, their stochastic model is known to a sufficient degree (Eueler and Goad, 1991, Satirapod and Wang, 2000), but this is not the case for ionospheric pseudo-observables. A small priori ionospheric standard deviation may result in the solutions with considerable biases, while a large one will cause ionosphere-weighted model lose effectiveness. A poor precision stochastic model may also affect the detection power of statistical tests. Investigations are needed to compare the performances of ionosphere-weighted model with different stochastic models.

In the following sections, the mathematical models of both conventional relative precise positioning and ionosphere-weighted model are given first. Since the observation noises of both pseudorange and carrier phase are elevation dependent, and also considering ionosphere delay from a lower satellite is usually larger than from satellite with a higher elevation. The exponential elevation weighting function is used to weight pseudorange, carrier phase and ionospheric pseudo-observables (Teunissen, 1997b). Subsequently, some experiments are conducted to demonstrate the performance of ionosphere-weighted model with different priori ionospheric standard deviations. The focus of this paper is to demonstrate the performance of ionosphere-weighted model with different ionospheric variances.

#### 2. Mathematical Models

The original DD pseudorange and carrier phase observations can be expressed as

$$\begin{split} P_{br,1}^{ij}(\mathbf{k}) &= \rho_{br}^{ij}(\mathbf{k}) + T_{br}^{ij}(\mathbf{k}) + \mu_{1}I_{br}^{ij}(\mathbf{k}) + \varepsilon_{P_{1}} \\ P_{br,2}^{ij}(\mathbf{k}) &= \rho_{br}^{ij}(\mathbf{k}) + T_{br}^{ij}(\mathbf{k}) + \mu_{2}I_{br}^{ij}(\mathbf{k}) + \varepsilon_{P2} \\ I_{br,1}^{ij}(\mathbf{k}) &= \rho_{br}^{ij}(\mathbf{k}) + T_{br}^{ij}(\mathbf{k}) - \mu_{1}I_{br}^{ij}(\mathbf{k}) + \lambda_{1}N_{br,1}^{ij} + \varepsilon_{L_{1}} \\ I_{br,2}^{ij}(\mathbf{k}) &= \rho_{br}^{ij}(\mathbf{k}) + T_{br}^{ij}(\mathbf{k}) - \mu_{2}I_{br}^{ij}(\mathbf{k}) + \lambda_{2}N_{br,1}^{ij} + \varepsilon_{L2} \end{split}$$

$$(1)$$

where  $P_{br}^{ij}$  and  $L_{br}^{ij}$  denote DD pseudorange and carrier phase in meters; subscripts b and r indicate base receiver and rover receiver, respectively; superscripts i and j denote satellite number; 1 and 2 are frequency indicators; k denotes the term of  $k^{th}$  epoch;  $\rho$  is the DD satellite-receiver range; T and I are tropospheric and ionosphere errors, respectively;  $\lambda_i$  is the wavelength of carrier phase;  $\mu_i$  is the frequency dependent ionospheric factor.

## 2.1 Ionosphere-weighted model

For the ionosphere-weighted model, the following equations are added to observation equations in (2).

$$I_{br,1}^{ij}(\mathbf{k}) = I_{br,1}^{ij}(\mathbf{k})$$
 (2)

For each satellite pair, one slant DD ionospheric pseudoobservable is added to the original observation equations to overcome the weak strength of estimating slant ionosphere parameters epoch by epoch (Teunissen, 1997a, Odijk, 2000, Odijk, 2002). In this study, the ionospheric pseudo-observables come from interpolated GIM (Schaer et al., 1998). For the reliability and accuracy of GIM, we can refer to e.g. (Hernández-Pajares et al., 2009).

The linearized geometry-based DD ionosphere-weighted functional model using dual-frequency pseudorange and phase observations of one epoch is shown in (3). For simplicity, subscripts and superscripts denoting receiver, satellite are omitted here. The epoch indicator is also dropped.

$$E\left\{\begin{bmatrix} P_{1} \\ P_{2} \\ L_{1} \\ L_{2} \\ I_{p} \end{bmatrix}\right\} = \begin{bmatrix} A & 0 & 0 & \mu_{1}I_{m} \\ A & 0 & 0 & \mu_{2}I_{m} \\ A & \lambda_{1}I_{m} & 0 & -\mu_{1}I_{m} \\ A & 0 & \lambda_{2}I_{m} & -\mu_{2}I_{m} \\ 0 & 0 & 0 & I_{m} \end{bmatrix} \begin{bmatrix} \Delta r \\ a_{1} \\ a_{2} \\ I \end{bmatrix}$$
(3)

Where E denotes the expectation operator; P and L are DD observation minus computation vectors of pseudorange and carrier phase, respectively;  $I_p$  denotes the residual DD ionospheric pseudo-observables on  $L_1$ ; matrix A is referred to as the geometry matrix of which contains the partial derivatives for baseline parameters;  $I_m$  is identity matrix, m denotes observation number of each observing type (m +1 satellite);  $a_1$  and  $a_2$  are DD integer ambiguities on  $L_1$  and  $L_2$  respectively; I denotes the unknown DD ionospheric delays on  $L_1$ .

#### 2.2 Elevation-Dependent stochastic model

Typical dependency of GNSS observation accuracy on their elevations can be expressed by the exponential function of satellite elevation angles (Teunissen, 1997b, Jin and Jong, 1996). As a result, the variance of undifferenced GNSS observable is proportional to

$$\sigma_r^s = (1 + c \exp^{-el_r^s/el_0})^2 \tag{4}$$

where c is a constant,  $el_0$  is a reference elevation angle.

After applying error propagation law to the original observations, the DD cofactor matrix with elevation weighting can be expressed as

$$Q = \begin{bmatrix} \sigma_{br}^{1} & \cdots & \sigma_{br}^{1} \\ \vdots & \ddots & \vdots \\ \sigma_{br}^{1} & \cdots & \sigma_{br}^{1} \end{bmatrix} + \begin{bmatrix} \sigma_{br}^{2} & & & \\ & \ddots & & \\ & & \sigma_{br}^{m+1} \end{bmatrix}$$
(5)

where  $\sigma_{br}^s = \sigma_b^s + \sigma_r^s$ , s = 1, ..., m+1. Here satellite 1 is assumed as the reference satellite and observations from rover and reference stations have different precisions. Assuming there is no correlation between different observation types. The stochastic model corresponding to equation (3) of one epoch with weighted ionospheric observations is written as

$$D_{y} = \begin{bmatrix} \sigma_{P_{1}}^{2} & & & & & \\ & \sigma_{P_{2}}^{2} & & & & \\ & & \sigma_{L_{1}}^{2} & & & \\ & & & \sigma_{L_{2}}^{2} & & \\ & & & & \sigma_{\iota}^{2} \end{bmatrix} \otimes Q \quad (6)$$

where  $\sigma_{P_1}, \sigma_{P_2}, \sigma_{L_1}, \sigma_{L_2}$  are standard deviations for undifferenced pseudorange and carrier phase on  $L_1$  and  $L_2$ .  $\sigma_i$  is the priori standard deviation for undifferenced ionospheric pseudo-observables. The same weighting method is applied to pseudorange, carrier phase and ionosphere. And  $\otimes$  is the kronecker product operator (Neudecker, 1969).

## 3. Numerical Analysis

## 3.1 Experiment description

To compare the performance of ionosphere-weighted model with ionosphere-fixed model, two baseline data sets were used in this experiment; see the detailed description in Table 1. Static baseline solutions were obtained using different length of data sessions, from 5 epochs to 720 epochs. The observational time is from 8:30am to 9:30am in GPS time on 12, August, 2013. The ground true baseline solution and integer ambiguity was obtained by processing 24 hours of static data. For ionosphere-fixed model, ionosphere delay was directly interpolated from the GIM model, while for ionosphereweighted model; ionosphere delay from GIM forms the pseudo-observable. The cut-off angle is set 20 degrees. Note that this paper mainly concentrates on ionospheric errors. In the following processing and analysis, tropospheric delay was corrected by Saastamoinen model with standard atmosphere.

Based on these data sets and processing options, a series of experiments were carried out to investigate the performance of ionosphere-weighted model and the impact of changing the priori ionospheric standard deviation. Their impacts on ambiguity resolution, mainly captured by F-ratio and W-ratio (Wang et al., 1998), and on final baseline components were given with different length of sessions. In the following analysis, three models are tested and compared.

- Model A: ionosphere-fixed model, ionosphere delay from GIM model is treated as true ionosphere error.
- **Model B**: ionosphere-weighted model with 2 mm ionosphere standard deviation.
- Model C: ionosphere-weighted model with 1 cm ionosphere standard deviation.

#### 3.2 Impact of weighting ionosphere

Table 2 summaries the F-ratio test results for baseline UNSW-MGRV with different length of sessions for the above three models. The first two rows are session length and number of epochs included. For model B and C, the standard deviation for undifferenced ionospheric pseudo-observables is set s 2mm and 1cm respectively. Comparing F-ratio values with model A, we can find that the ratio value is generally increased when observation length is less than 5 minutes after weighing the ionosphere. However for longer sessions, this trend disappears. Table 3 is ambiguity validation results by the F-ratio test for the longer baseline VLWD-NWRA. The F-ratio indicates that in most cases, model B and C perform better than model A even for long observation cases. And also model B is slightly better than model C here. This might suggest that a 2mm weighting of ionosphere might be better than 1cm in this situation. From above analysis, we can find that weighting ionosphere can really affect the reliability of ambiguity resolution. Similar results were observed using W-ratio (Wang et al, 1998).

**Table 4** to **Table 6** shows the coordinate difference in north, east and up components, respectively, from UNSW to MGRV with different length of sessions. The reference solution is obtained by processing 24 hours static data. The first Table shows the accuracy without weighting Ionosphere. The GIM is used here to account for ionospheric delays on both stations, while in **Table 5** and **Table 6**, 2mm and 1cm priori standard deviation is given to weight the ionospheric pseudo-observables.

Table 1: Data sets description

| Data Set | et   Data Span   Interval |       | <b>Baseline Length</b> | Date       | Location  |
|----------|---------------------------|-------|------------------------|------------|-----------|
| a        | 60 min                    | 5 sec | 49 km                  | 12/08/2013 | UNSW-MGRV |
| b        | 60 min                    | 5 sec | 115 km                 | 12/08/2013 | VLWD-NWRA |

Table 2: Ambiguity validation results by the F-ratio test for baseline UNSW-MGRV

| obs. length(sec) | 25  | 50  | 150 | 300 | 600 | 1200 | 1800 | 2400 | 3000 | 3600 |
|------------------|-----|-----|-----|-----|-----|------|------|------|------|------|
| epoch            | 5   | 10  | 30  | 60  | 120 | 240  | 360  | 480  | 600  | 720  |
| Model A          | 1.3 | 1.5 | 1.9 | 2.0 | 3.0 | 4.0  | 4.5  | 5.6  | 6.0  | 6.1  |
| Model B          | 2.6 | 2.7 | 2.9 | 2.8 | 2.7 | 2.8  | 3.2  | 3.7  | 4.3  | 4.7  |
| Model C          | 3.0 | 2.9 | 2.6 | 2.9 | 2.7 | 2.5  | 2.6  | 3.0  | 3.4  | 3.7  |

Table 3: Ambiguity validation results by the F-ratio test for baseline VLWD-NWRA

| obs. length(sec) | 25  | 50  | 150 | 300 | 600 | 1200 | 1800 | 2400 | 3000 | 3600 |
|------------------|-----|-----|-----|-----|-----|------|------|------|------|------|
| epoch            | 5   | 10  | 30  | 60  | 120 | 240  | 360  | 480  | 600  | 720  |
| Model A          | 1.1 | 1.0 | 1.5 | 1.2 | 1.7 | 2.6  | 2.1  | 2.0  | 2.1  | 1.9  |
| Model B          | 1.1 | 1.1 | 1.2 | 1.4 | 1.7 | 2.5  | 2.6  | 2.4  | 2.5  | 2.4  |
| Model C          | 1.1 | 1.0 | 1.1 | 1.1 | 1.5 | 2.1  | 2.3  | 2.5  | 2.4  | 2.4  |

Table 4: Coordinate difference for baseline UNSW-MGRV with model A

| obs. length(sec) | 25     | 50     | 150    | 300    | 600    | 1200  | 1800   | 2400   | 3000   | 3600   |
|------------------|--------|--------|--------|--------|--------|-------|--------|--------|--------|--------|
| epoch            | 5      | 10     | 30     | 60     | 120    | 240   | 360    | 480    | 600    | 720    |
| north(m)         | 0.053  | 0.049  | 0.034  | 0.020  | 0.008  | 0.008 | 0.009  | 0.010  | 0.014  | 0.023  |
| east(m)          | -0.221 | -0.022 | -0.016 | -0.011 | -0.005 | 0.000 | 0.002  | 0.001  | -0.001 | -0.004 |
| up(m)            | 0.009  | 0.007  | 0.015  | 0.000  | -0.007 | 0.002 | -0.001 | -0.005 | -0.012 | -0.012 |

Table 5: Coordinate difference for baseline UNSW-MGRV with model B

| obs. length(sec) | 25     | 50     | 150    | 300    | 600    | 1200   | 1800   | 2400   | 3000   | 3600   |
|------------------|--------|--------|--------|--------|--------|--------|--------|--------|--------|--------|
| epoch            | 5      | 10     | 30     | 60     | 120    | 240    | 360    | 480    | 600    | 720    |
| north(m)         | 0.066  | 0.060  | 0.045  | 0.033  | 0.026  | 0.028  | 0.026  | 0.026  | 0.027  | 0.032  |
| east(m)          | -0.035 | -0.035 | -0.030 | -0.025 | -0.022 | -0.018 | -0.014 | -0.013 | -0.014 | -0.016 |
| up(m)            | 0.000  | 0.000  | 0.012  | 0.003  | 0.001  | 0.007  | 0.004  | -0.001 | -0.007 | -0.008 |

Table 6: Coordinate difference for baseline UNSW-MGRV with model C

| obs. length(sec) | 25     | 50     | 150    | 300    | 600    | 1200   | 1800   | 2400   | 3000   | 3600   |
|------------------|--------|--------|--------|--------|--------|--------|--------|--------|--------|--------|
| epoch            | 5      | 10     | 30     | 60     | 120    | 240    | 360    | 480    | 600    | 720    |
| north(m)         | 0.084  | 0.077  | 0.062  | 0.052  | 0.051  | 0.056  | 0.051  | 0.048  | 0.046  | 0.046  |
| east(m)          | -0.054 | -0.054 | -0.049 | -0.046 | -0.046 | -0.042 | -0.037 | -0.034 | -0.034 | -0.033 |
| up(m)            | -0.012 | -0.011 | 0.006  | 0.008  | 0.012  | 0.014  | 0.012  | 0.005  | 0.000  | -0.001 |

The above tables show that centimetre accuracy can be achieved whether ionosphere is weighted for this shorter baseline (49km). And the coordinate difference with model B is overall smaller than model C, which might indicate a 2mm weight for ionosphere is more appropriate than 1 cm in this case. However, the unexpected 22cm positioning error in east direction with 5 epochs of model A disappeared when ionosphere is weighted.

Table 7 to Table 9 shows the coordinate difference in north, east and up components, respectively, from VLWD to NWRA with different length of observations processed with model A, B and C. The reference solution was obtained by processing 24 hours static data.

It's shown that for this over 115 km baseline, the positioning biases can reach up to several meters without weighting the ionosphere if observation length is less than 5 minutes. These biases still exist in model C. However, there is significant improvement in model B, which weights the ionosphere with 2mm. For longer observations, any of these three models can achieve cm accuracy. Comparing with the previous 49km baseline, the improvement of weighting ionosphere is more significant for longer baseline. The two baseline experiments may suggest positioning accuracy is more consistent if ionosphere weighting is applied even in short observation cases. In the following section, we will investigate the impact of varying the ionosphere variance.

|                  | Table 7: Coordinate difference for baseline VLWD-NWRA with model A |        |        |        |        |        |        |        |        |        |  |  |  |
|------------------|--|--------|--------|--------|--------|--------|--------|--------|--------|--------|--|--|--|
| obs. length(sec) | 25   | 50     | 150    | 300    | 600    | 1200   | 1800   | 2400   | 3000   | 3600   |  |  |  |
| epoch            | 5  | 10     | 30     | 60     | 120    | 240    | 360    | 480    | 600    | 720    |  |  |  |
| north(m)         | 3.740  | -3.666 | -0.465 | -0.440 | 0.018  | 0.025  | 0.029  | 0.015  | 0.006  | -0.007 |  |  |  |
| east(m)          | -0.175   | -0.112 | 0.122  | 0.117  | -0.034 | -0.038 | -0.044 | -0.048 | -0.048 | -0.047 |  |  |  |
| up(m)            | 0.016  | -0.611 | -0.228 | -0.237 | 0.015  | -0.001 | -0.007 | -0.008 | -0.013 | -0.024 |  |  |  |

Table 7: Coordinate difference for baseline VLWD-NWRA with model A

Table 8: Coordinate difference for baseline VLWD-NWRA with model B

| obs. length(sec) | 25     | 50     | 150    | 300    | 600    | 1200   | 1800   | 2400   | 3000   | 3600   |
|------------------|--------|--------|--------|--------|--------|--------|--------|--------|--------|--------|
| epoch            | 5      | 10     | 30     | 60     | 120    | 240    | 360    | 480    | 600    | 720    |
| north(m)         | -0.038 | -0.036 | -0.040 | -0.032 | -0.024 | -0.016 | -0.011 | -0.019 | -0.023 | -0.031 |
| east(m)          | -0.022 | -0.024 | -0.024 | -0.026 | -0.033 | -0.036 | -0.041 | -0.044 | -0.045 | -0.044 |
| up(m)            | -0.014 | -0.013 | -0.005 | -0.002 | -0.003 | -0.015 | -0.020 | -0.023 | -0.027 | -0.035 |

Table 9: Coordinate difference for baseline VLWD-NWRA with model C

| obs. length(sec) | 25     | 50     | 150    | 300    | 600    | 1200   | 1800   | 2400   | 3000   | 3600   |  |  |
|------------------|--------|--------|--------|--------|--------|--------|--------|--------|--------|--------|--|--|
| epoch            | 5      | 10     | 30     | 60     | 120    | 240    | 360    | 480    | 600    | 720    |  |  |
| north(m)         | -0.099 | -0.351 | -0.343 | -0.086 | -0.084 | -0.075 | -0.069 | -0.068 | -0.065 | -0.066 |  |  |
| east(m)          | -0.023 | 0.054  | 0.051  | -0.029 | -0.031 | -0.033 | -0.036 | -0.038 | -0.040 | -0.040 |  |  |
| up(m)            | -0.023 | -0.144 | -0.149 | -0.029 | -0.031 | -0.036 | -0.040 | -0.045 | -0.048 | -0.051 |  |  |

Table 7 to Table 9 shows the coordinate difference in north, east and up components, respectively, from VLWD to NWRA with different length of observations processed with model A, B and C. The reference solution was obtained by processing 24 hours static data. It's shown that for this over 115 km baseline, the positioning biases can reach up to several meters without weighting the ionosphere if observation length is less than 5 minutes. These biases still exist in model C. However, there is significant improvement in model B, which weights the ionosphere with 2mm. For longer observations, any of these three models can achieve cm accuracy. Comparing with the previous 49km baseline, the improvement of weighting ionosphere is more significant for longer baseline. The two baseline experiments may suggest positioning accuracy is more consistent if ionosphere weighting is applied even in short observation cases. In the following section, we will investigate the impact of varying the ionosphere variance.

## 3.3 Varying Ionosphere variance

To make the best use of ionosphere-weighted model, an appropriate model for ionosphere variance should be chosen for this parameter. Too optimistic variance models will most likely result in an incorrect estimation of the carrier phase ambiguities and thus incorrect position while too pessimistic variance models will lower the availability of a position solution due to the inability to estimate the carrier phase ambiguities. The ionosphere variance should not be chosen arbitrarily. **Figure 1** and **Figure 2** show estimated DD ionospheric delay of 360 consecutive epochs for baseline VLWD-

NWRA with both model B and model C. These are actually residual delays corrected by GIM model. For model B, 2mm standard deviation was given to the ionospheric pseudo-observables; while in model C it was set as 1cm. Different colours indicate different PRN pairs. In both cases, satellite 13 with the highest elevation angle was chosen as reference satellite. As shown in both figures, the residual DD ionospheric delay varies within 4 cm. In both cases, the mean residual delay of each satellite pair is close to zero. However, the variation of model C is slightly larger than model B.

We have calculated the standard deviation of estimated ionosphere (STD IONO) time series for both models, shown in Table 10 and Table 11. For validation purpose, we also provided the squared diagonal elements of ionosphere covariance matrix (STD\_COV), which were constructed from priori ionosphere variance after applying satellite elevation-weighting and the doubledifferencing. The variance of estimated ionosphere delay is expected to reflect the variance of ionospheric pseudoobservables, which means the values of STD IONO and STD COV should be close to each other if the priori variance of ionosphere is chosen appropriately. Table 10 shows a good agreement between these two variables, while in Table 11, there is significant difference between them. This finding may suggest that for this over 115km baseline, a 2mm standard deviation for ionospheric pseudo-observables is more appropriate than a 1cm one. This conclusion is also confirmed by comparing the result of Table 8 and Table 9 that model B performs better than model C.

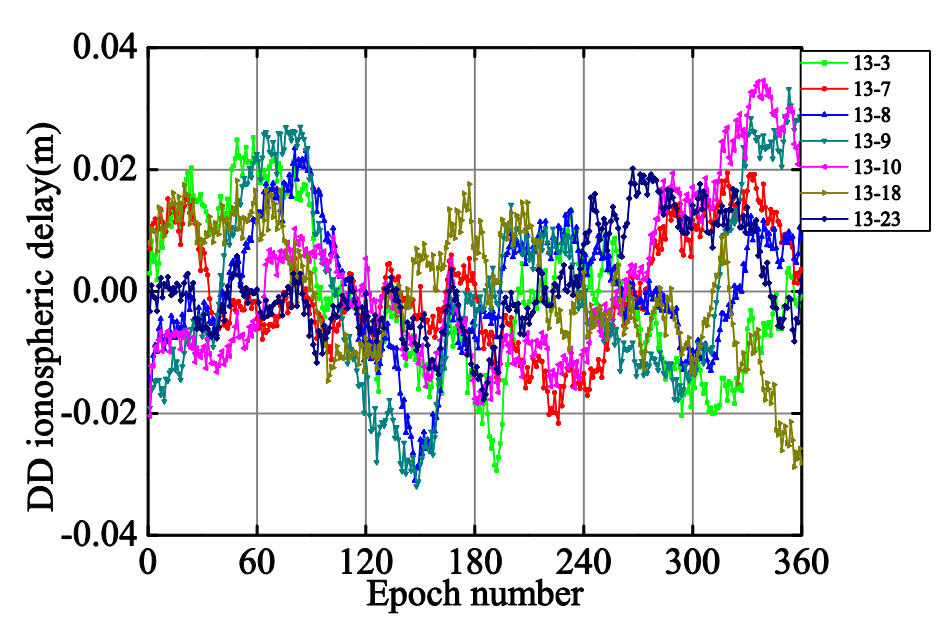


Figure 1: DD ionospheric delays for baseline VLWD-NWRA with model B

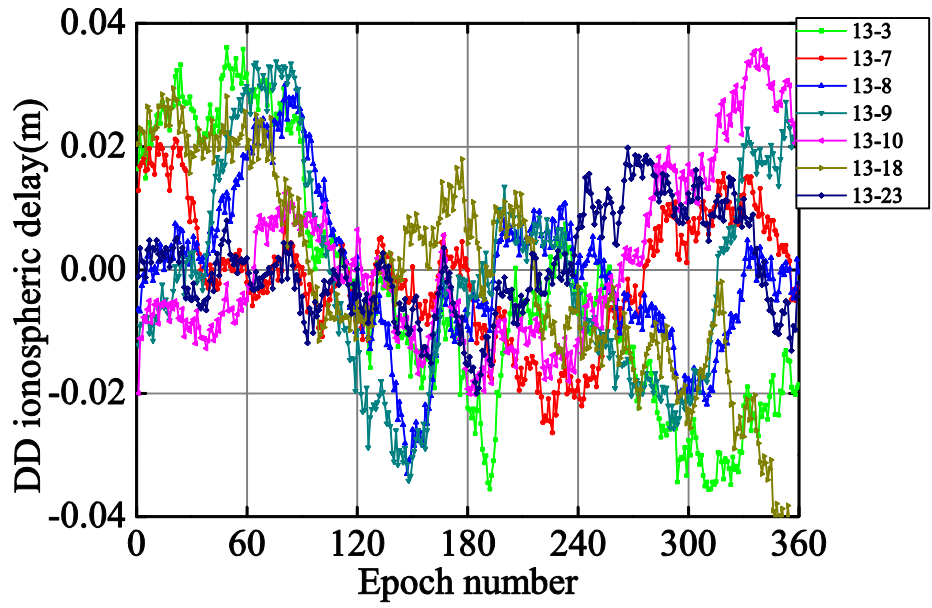


Figure 2: DD ionospheric delays for baseline VLWD-NWRA with model C

Table 10: STD\_IONO and STD\_COV for VLWD-NWRA with model B

| PRN pair    | 13-3  | 13-7  | 13-8  | 13-9  | 13-10 | 13-18 | 13-23 |
|-------------|-------|-------|-------|-------|-------|-------|-------|
| STD_IONO(m) | 0.012 | 0.009 | 0.010 | 0.016 | 0.013 | 0.010 | 0.008 |
| STD_COV(m)  | 0.012 | 0.008 | 0.012 | 0.013 | 0.010 | 0.014 | 0.008 |

Table 11: STD IONO and STD COV for VLWD-NWRA with model C

| PRN pair    | 13-3  | 13-7  | 13-8  | 13-9  | 13-10 | 13-18 | 13-23 |  |  |  |  |
|-------------|-------|-------|-------|-------|-------|-------|-------|--|--|--|--|
| STD_IONO(m) | 0.020 | 0.010 | 0.013 | 0.017 | 0.014 | 0.017 | 0.008 |  |  |  |  |
| STD_COV(m)  | 0.059 | 0.038 | 0.059 | 0.064 | 0.052 | 0.070 | 0.040 |  |  |  |  |

## 4. Concluding Remarks

The performance of ionosphere-weighted model with elevation-dependent weighting and the impact of varying priori ionospheric standard deviation on ambiguity resolution and baseline solution have been presented and discussed in this paper. The results shows that, the ionosphere-weighted model can indeed improve the reliability of ambiguity resolution, especially when observation session length is short, e.g. less than 5 minutes. And for longer baselines, the improvement in positioning performance is more significant compared with a shorter baseline. To fully exploit ionosphereweighted model, neither a too optimistic nor too pessimistic variance model should be chosen. addition, in this paper we have analysed the standard deviation of estimated ionosphere time series to validate correctness of preselected ionosphere variance. More investigations are needed to determine a realistic ionosphere variance parameter. The future work may consider using some estimation methods to estimate ionosphere variance.

## Acknowledgments

The first author would like to acknowledge CORSnet-NSW for providing data sets for this research.

#### References

- Alves, P., Lachapelle, G., Cannon, M. E., Park, J. & Park, P. Use of self-contained ionospheric modeling to enhance long baseline multiple reference station RTK positioning. Proceedings of the Institute of Navigation 2002 meeting, 2002.
- Eueler, H.-J. & Goad, C. 1991. On optimal filtering of GPS dual frequency observations without using orbit information. *Bulletin géodésique*, 65, 130-143.
- Hernández-Pajares, M., Juan, J. M., Sanz, J., Orus, R., Garcia-Rigo, A., Feltens, J., Komjathy, A., Schaer, S.
  C. & Krankowski, A. 2009. The IGS VTEC maps: a reliable source of ionospheric information since 1998. *Journal of Geodesy*, 83, 263-275.
- Hu, G., Abbey, D. A., Castleden, N., Featherstone, W. E., Earls, C., Ovstedal, O. & Weihing, D. 2005. An approach for instantaneous ambiguity resolution for medium- to long-range multiple reference station networks. GPS Solutions, 9, 1-11.
- Jin, X.-X. & Jong, C. D. d. 1996. Relationship between satellite elevation and precision of GPS code observations. *Journal of Navigation*, 49, 253-265.

- Klobuchar, J. A. 1987. Ionospheric Time-Delay Algorithm for Single-Frequency GPS Users. *Transactions on Aerospace and Electronic Systems*, AES-23, 325-331.
- Liu, G. C. H. 2001. *Ionosphere weighted global positioning system carrier phase ambiguity resolution*. University of Calgary, Department of Geomatics Engineering.
- Mannucci, A. J., Wilson, B. D., Yuan, D. N., Ho, C. H., Lindqwister, U. J. & Runge, T. F. 1998. A global mapping technique for GPS-derived ionospheric total electron content measurements. *Radio Science*, 33, 565-582.
- Marques, H. A., Monico, J. F. G. & Aquino, M. 2011. RINEX\_HO: second- and third-order ionospheric corrections for RINEX observation files. *GPS Solutions*, 15, 305-314.
- Neudecker, H. 1969. A Note on Kronecker Matrix Products and Matrix Equation Systems. *SIAM Journal on Applied Mathematics*, 17, 603-606.
- Odijk, D. Weighting ionospheric corrections to improve fast GPS positioning over medium distances. Proceedings of the Institute of Navigation 2000 meeting, 2000.
- Odijk, D. 2002. Fast precise GPS positioning in the presence of ionospheric delays. Dissertation, Delft University of Technology.
- Satirapod, C. & Wang, J. 2000. Comparing the quality indicators of GPS carrier phase observations. *Geomatics Research Australasia*, 73, 75-92.
- Schaer, S. 1999. Mapping and predicting the Earth's ionosphere using the Global Positioning System. *Geod.-Geophys. Arb. Schweiz, Vol. 59*, 59.
- Schaer, S., Beutler, G., Mervart, L., Rothacher, M. & Wild, U. Global and regional ionospheric models using the gps double difference phase observable. IGS Workshop Proceedings on Special Topics and New Directions, 1995 GFZ, Potsdam, Germany. 77-92.
- Schaer, S., Gurtner, W. & Feltens, J. IONEX: The ionosphere map exchange format version 1. 1998.
- Takasu, T. & Yasuda, A. Kalman-filter-based integer ambiguity resolution strategy for long-baseline RTK with ionosphere and troposphere estimation. ION NTM, 2010.

- Teunissen, P. J. G. 1997a. The geometry-free GPS ambiguity search space with a weighted ionosphere. *Journal of Geodesy*, 71, 370-383.
- Teunissen, P. J. G. 1997b. On the sensitivity of the location, size and shape of the GPS ambiguity search space to certain changes in the stochastic model. *Journal of Geodesy*, 71, 541-551.
- Wang, J., Stewart, M. P. & Tsakiri, M. 1998. A discrimination test procedure for ambiguity resolution on-the-fly. *Journal of Geodesy*, 72, 644-653.
- Wielgosz, P. 2011. Quality assessment of GPS rapid static positioning with weighted ionospheric parameters in generalized least squares. *GPS Solutions*, 15, 89-99.

#### **Biography**

Jinling Wang is an Associate Professor in the School of Civil and Environmental Engineering, University of New South Wales (UNSW). His major research interests are in the areas of navigation and geospatial mapping with multi-sensors, such as GNSS, INS, cameras. He has

published over 200 papers in journals and conference proceedings as well as two commercial software packages (see more details of the research activities within his team at www.gmat.unsw.edu.au/wang). He is a Fellow of the Royal Institute of Navigation (RIN), UK, a Fellow of the International Association of Geodesy (IAG), and is a member of the Editorial Board for the international journal GPS Solutions, Journal of Navigation, International Journal of Navigation and Observations, and President of IAG Sub-Commission 4.2 (2011-2015) on Geodesy in Geospatial Mapping and Engineering. He was elected 2004 President of the International Association of Chinese Professionals in Global Positioning Systems (CPGPS), and the Founding Editor-in-Chief for the Journal of Global Positioning Systems (2002-2007).

Peiyuan Zhou is currently a Ph.D. student in the School of Civil and Environmental Engineering, University of New South Wales (UNSW). He obtained his B.Sc. degree (2012) in School of Geodesy and Geomatics from Wuhan University, China. His main research focuses on ionosphere modelling and stochastic modelling in precise GNSS positioning.